

Solar Cell Nanotechnology for Improved Efficiency and Radiation Hardness

Alexander I. Fedoseyev ^{a*}, Marek Turowski ^a, Qinghui Shao ^b and Alexander A. Balandin ^b

^aCFD Research Corporation (CFDRC), 215 Wynn Drive, Huntsville, AL 35805

^bNano-Device Laboratory, Department of Electrical Engineering, UC-Riverside, CA 92521

ABSTRACT

Space electronic equipment, and NASA future exploration missions in particular, require improvements in solar cell efficiency and radiation hardness. Novel nano-engineered materials and quantum-dot array based photovoltaic devices promise to deliver more efficient, lightweight solar cells and arrays which will be of high value to long term space missions. In this paper, we describe issues related to the development of the quantum-dot based solar cells and comprehensive software tools for simulation of the nanostructure-based photovoltaic cells. Some experimental results used for the model validation are also reviewed. The novel modeling and simulation tools for the quantum-dot-based nanostructures help to better understand and predict behavior of the nano-devices and novel materials in space environment, assess technologies, devices, and materials for new electronic systems as well as to better evaluate the performance and radiation response of the devices at an early design stage. The overall objective is to investigate and design new photovoltaic structures based on quantum dots (QDs) with improved efficiency and radiation hardness. The inherently radiation tolerant quantum dots of variable sizes maximize absorption of different light wavelengths, *i.e.*, create a “multicolor” cell, which improves photovoltaic efficiency and diminishes the radiation-induced degradation. The QD models described here are being integrated into the advanced photonic-electronic device simulator NanoTCAD, which can be useful for the optimization of QD superlattices as well as for the development and exploring of new solar cell designs.

Keywords: solar cell, quantum dot, nanostructures, photovoltaic, radiation tolerant, computer-aided-design

1. INTRODUCTION

In the high-radiation open space environment the solar cells suffer from degradation, which depends on the materials and particular design of the photovoltaic cells (Figure 1). Despite previous studies of the performance of solar cells in the radiation environment [1, 32, 37], the exact mechanisms of the radiation-induced degradation have not been accurately established. Substantial work has been performed on the radiation hardening of the space electronics while much less attention has been devoted to the solar arrays, which are crucial to the operation of an entire spacecraft.

The issue of the solar cell radiation hardness can be addressed at a number of levels. One possible approach is to use improvements in the material quality, design, or manufacturing process for incremental enhancement of the radiation hardness of the solar cells fabricated with conventional technology. Our current approach is based on recent nanotechnology breakthroughs, which led to emergence of the quantum dot superlattice (QDS) structures. QDS structures offer additional degrees of freedom in tuning the photon absorption and the photogenerated carrier transport through the effects of quantum confinement and spatial confinement of the phonon modes. The theoretical studies predicted a potential solar cell efficiency of around 63%, which is approximately a factor of two better than any state-of-the-art devices available today [4, 38]. The joint CFDRC and UC-Riverside group is currently developing a comprehensive software tool, which would allow to design and optimize QDS and other nanostructures for increasing the efficiency and radiation tolerance (Figure 2). The availability of such tool is important for guiding the experimental developments and achieving faster progress in the solar cell technology.

*Corresponding author; electronic mail: aif@cfdrc.com, phone: (256)726-4928; fax: (256)726-4806; www.cfdrc.com

The semiconductor quantum dots (QDs) are expected not only to improve the photovoltaic (PV) efficiency, by expanding the spectral response of the individual cells, but also the radiation tolerance. The inherently more radiation tolerant QDs can be used to take advantage of the thermal assist in the carrier generation. This is important owing to the attempts of increasing the array-specific power with the new concentrator designs and continuing expansion of the range of environments to be encountered in future missions.

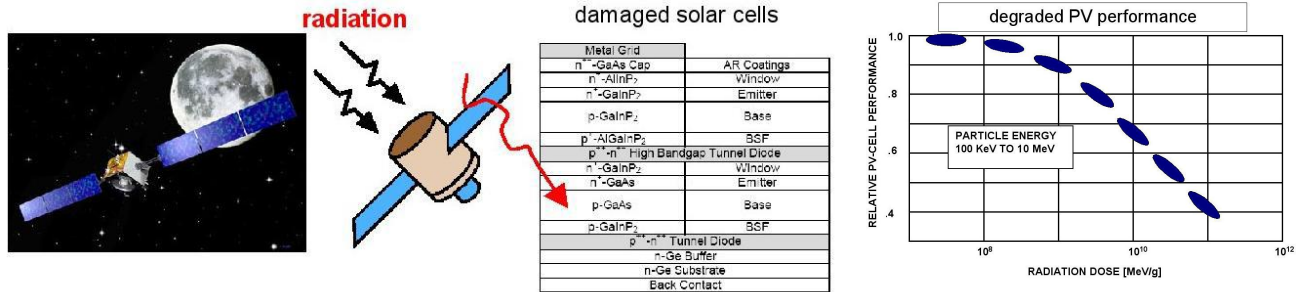


Figure 1. Solar cells, which are the basis of the power supply systems in space, degrade under the space radiation environment depending on the materials and design of the photovoltaic (PV) cells (right plot shows a typical degradation trend, after [32]).

The reported observations for several optoelectronic devices with QDs in the active area show the increased radiation tolerance. For instance, it has been demonstrated [29] that QD-based structures are inherently more radiation tolerant due to the effects of three dimensional quantum confinement. An increase in the radiation hardness of as much as two orders of magnitude has been obtained by comparisons with the quantum wells of the same composition and placed at the same depth in the structure [29].

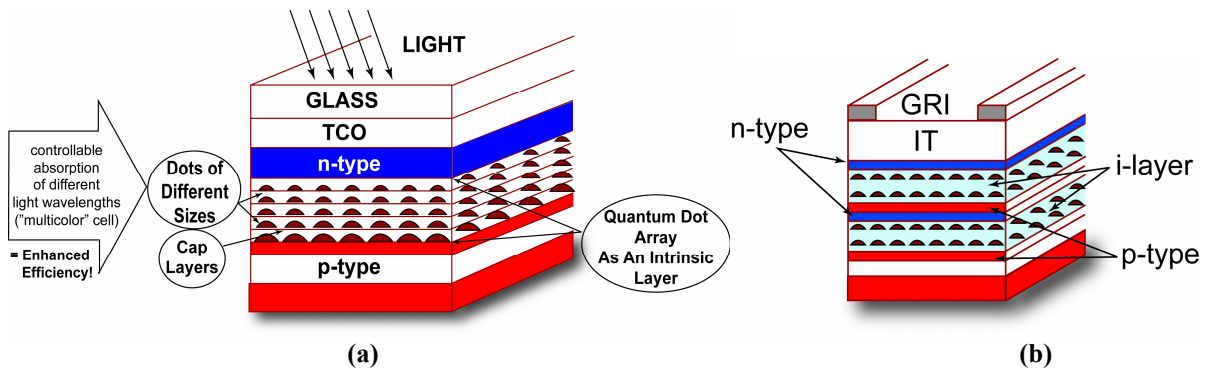


Figure 2. Schematic structure of the PV cell based on the quantum dot superlattice (QDS), which is used as a prototype for the development of the PV cell simulation tools. The structure contains a stack of multiple quantum-dot arrays with the variable dot size, which maximizes absorption of the different light wavelengths in a controllable way, i.e., creates a “multicolor” cell. The inset shows another possible design – a multiple junction cell.

The modeling-based optimization of the nanostructured materials and devices is crucial for the development of novel solar cells. This requires reliable computer modeling tools for analysis, performance estimation, and optimization, which includes the simulation of the charge carriers, phonon states, electron – phonon scattering rates and photon absorption in semiconductor nanostructures. Currently, there are no professional, reliable software tools available for this purpose despite the fact that incorporation of nanoscale physical phenomena in a proper way is essential for the design optimization of such quantum devices.

The advantages of the solar cells nanotechnology, which can be developed with the help of the modeling-based nanostructure optimization, include the following. The QD solar cells can be much more efficient than the traditional multi-layer solar cells resulting in the increased capacity of the solar array at the beginning of life (BOL). The increased BOL capacity will compensate for the degradation (including the radiation from natural and man-made sources), so that the end of life (EOL) capacity will also increase. The QD structures are inherently more radiation tolerant (with predicted increase in the radiation hardness of as much as two orders of magnitude compared to the quantum-well structures). The fine-tuning of the charge carrier transport in nanostructures using the confinement effects can lead to further enhancement of the efficiency and radiation hardness. At the same time, the theoretically predicted improvements in PV technology can be implemented only if the nanostructures are optimized. Thus, the computer modeling tools, which include simulation of the carriers, confined acoustic and optical phonons and photon absorption in semiconductor QDS, are essential for PV nanotechnology development.

2. PHYSICAL MODELING OF THE QUANTUM DOT PHOTOVOLTAIC CELLS

As a prototype structure for the modeling-based optimization we consider QDS-based PV cell (see Figure 2). The basic element of this PV cell is a stack of quantum dots arrays, referred to as QDS. The QDS can be implemented on Si/Ge or other material systems including III-Vs group materials such as GaAs. The QDS forms an intrinsic layer in a regular n-i-p (p-i-n) solar cell configuration. Quantum confinement of charge carriers (electrons and holes) in variable-size quantum dots, which form the i-layer, increases the effective band gap of the material and improves the absorption characteristics of the material system. The increased oscillator strength of the inter-band transitions due to size effects and modified density of states allow one to enhance light absorption and, potentially, the PV efficiency. The vertical arrangement of quantum dots, i.e., one on top of the other one, small inter-dot distance, crystallinity of the material and absence of defects present in conventional amorphous-silicon (a-Si) PV cells, allow one to maintain a high electric conductivity. The latter, together with the optimized $\mu\tau$ product in the growth direction (here μ is the carrier mobility, and τ is the carrier recombination lifetime), is expected to lead to the enhanced PV performance. The quantum dot size variation allows one to optimize absorption at different wavelengths and create a *multicolor* quantum PV cell with estimated efficiency greater than 40%.

The practical realization of this nanostructure-based PV cell depends on the successful computer-aided optimization of the structure parameters and solution of a number of technological problems. Some of the addressed problems are (i) finding the optimum match between the electron (hole) diffusion length and the thickness of the *p* (*n*) region; (ii) calculation and measurement of the mean optical penetration depth and electrical conductivity in QDS structures; and (iii) low-cost fabrication of the high-quality QDS with the low defect densities and desired dot regimentation. Since the proposed structure is drastically different from the conventional PV cells, based on amorphous-silicon (a-Si), crystalline silicon (c-Si), or nanocrystalline silicon (nc-Si), the known characteristic values of the PV cell parameters are not valid in this case and cannot be used in the modeling.

2.1. Rationale for the QD Photovoltaic Cell Concept

It has been shown that utilization of the nanocrystalline silicon (nc-Si) as an intrinsic layer in thin film n-i-p solar cells can bring about significant improvement of the efficiency [11, 21]. The improvement has been attributed to the quantum confinement of carriers, which leads to the increase of the effective band gap, and allows one to achieve strong absorption in nc-Si. At the same time, disorder and many structural defects characteristic to nc-Si and a-Si materials lead to large densities of recombination centers that hamper the operation of photovoltaic cells. Many defects, e.g., dangling bonds, weak bonds, and other trapping centers, which are present in disordered materials such as nc-Si or a-Si do not allow one to fully utilize benefits of quantum confinement of carriers and other low-dimensional phenomena. The QDS-based PV cells can avoid problems typically associated with disordered a-Si or nc-Si materials, yet allow one to use the benefits of quantum confinement. These benefits can be realized through improvements in a number of processes as summarized below.

2.2. Principle of the QD Photovoltaic Cell Operation

In its simplest form the quantum dot photovoltaic (QDPV) cell consists of a single-junction *n-i-p* cell with the structure similar to the currently used microcrystalline silicon (mc-Si:H) thin-film cells or a-Si cells. The principal difference and novelty lie in the design of the intrinsic layer (i-layer, Figure 2). The i-layer utilizes QDS, with the vertical correlation of the dot positions and variable dot size. MBE self-assembly technique can be used to fabricate prototype QD photovoltaic structures with the following features: (i) the stack of up to 100 quantum dots arrays with the layer thickness $W = 10$ nm to 50 nm each; (ii) the dot size is variable from 4 nm to 40 nm; (iii) the dot shape is intermediate between the sphere and disk-like; and (iv) the thickness of the active layer (top *n*-type layer and i-layer) kept at ~ 1 μm . The parameters of the growth process can be adjusted in such a way that the dot position in each consecutive layer is correlated with the dot site in the previous layer; the dots grow on top of each other. Moreover, the size of the quantum dots in each consecutive layer is slightly bigger than in the previous one, and the effective band-gap is correspondingly smaller (see Figure 3). Such variations in size and vertical site correlation are achieved using the Stravinski-Krastanov MBE growth mode with specially chosen conditions (temperature, deposition rate, etc.). The quality and crystallinity of quantum dots can be very high [30].

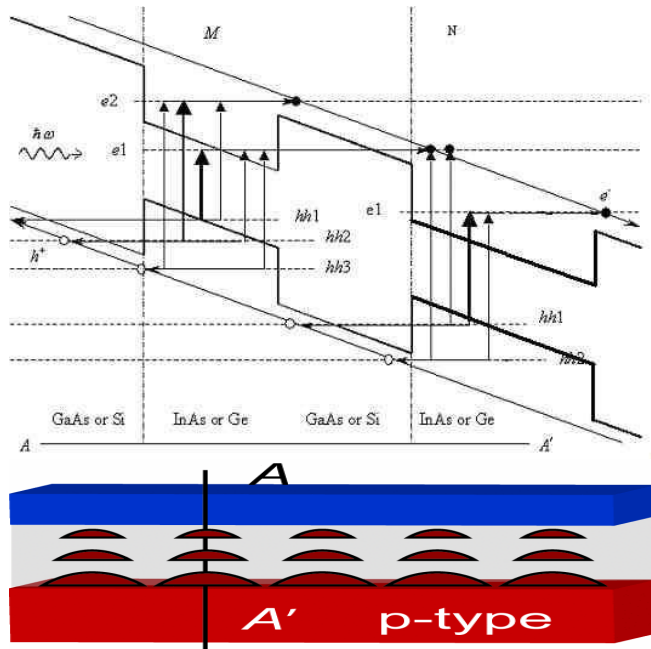


Figure 3. Schematic of the band structure and quantum-dot layers system arrangement along vertical line AA'. Confinement of the electrons (holes) in the semiconductor quantum dots increases the oscillator strength of the transitions between the electron (hole) states and the continuum electron (hole) states, thus enhancing the absorption. The different dots sizes lead to maximizing the absorption at the different energies (photon wavelength): E_{h1} transition energy (effective band-gap) is smaller for dot N than for dot M. Photogenerated holes and electrons are swept by the built-in field and collected by the corresponding contacts. The electron (hole) current consists of the continuum state component and the tunneling (below-the-barrier) component due to the barrier wave-function overlap between the confined states.

Based on the preliminary investigation at UCR NDL, it is expected that the diffusion length in the cross-plane direction of Si/Ge QDS is on the order of 1 μm [9], larger than that for nc-Si and mc-Si. Thus, the drift-assisted collection of the photogenerated carriers through the photovoltaically active intrinsic QDS layer is possible. The *n-i-p* structure can be replaced with a *p-i-n* structure, depending on the performance and technological considerations. The proposed scheme has been extended to a more complicated multiple-junction design (Figure 2, inset), which is expected to have even higher efficiency.

Figure 3 illustrates the band structure and optical transitions between the confined valence and continuum conduction band states. In Ge QDs grown on Si (100), almost all the band-gap offset goes to the valence band, although one can introduce a conduction band offset by growing part of the structure on SiC substrate so that Si layers are under tensile strain. In InAs QDs grown on GaAs the band offset splits between the conduction and valence bands. In the considered design, a conventional transparent conductive oxide (TCO) for the PV cell is used. ZnO or doped SnO₂ fabricated by various methods such as low pressure CVD or sputtering are compatible with proposed MBE grown QDS structure. The

use of ZnO is preferable since it offers superior transparency and higher chemical stability. The two important physical phenomena affecting PV-cell performance, which are incorporated into our modeling, are described below.

2.3. Analysis of Light Trapping and Absorption

One of the important advantages of the QDS PV cell, as compared to the bulk material PV cell, is the light trapping and absorption ability that comes with nanostructured material. The layer of QDs with the feature sizes smaller than the light wavelength serves as an effective scatterer, which helps in trapping the incident light (see Figure 4). The incident light wave scattered by the inside layer of quantum dots is then repeatedly scattered by the adjacent layers, gets trapped and eventually absorbed. The strength of optical transitions is determined by the inter-band dipole matrix element ($|e_{cv}|^2$), the electron-hole (e-h) envelope function overlap, and the joint density of states [51]. The quasi-3D quantum confinement in QDs increases the electron-hole wave-function overlap as well as the density of states (DOS), thus leading to stronger absorption and more effective photogeneration of carriers. The process of the initial light trapping is somewhat similar to the one in PV cells with rough back reflectors and TCO/a-Si interface but it is more effective due to the presence of multiple layers of QDs. Other factors, which may lead to the improvement of the light trapping, are the high reflectance of the doped substrate and rear metal contact as well as low absorption at the glass coating – TCO interface (see Eq. (1)). One should also mention that the nanostructure-based PV cell does not require texturing for improving the light trapping, thus reducing one extra fabrication step.

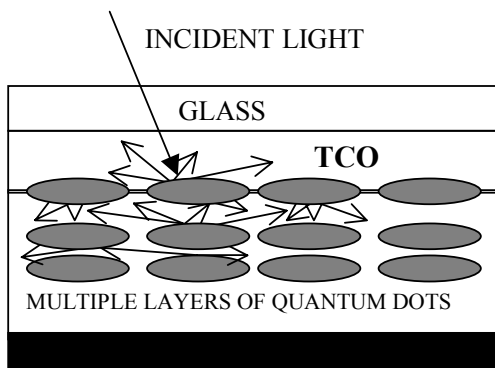


Figure 4. Illustration of the light trapping mechanism in a QD PV cell. The incident light is scattered by multiple layers of quantum dots, reflected, trapped inside cap layers, and eventually absorbed.

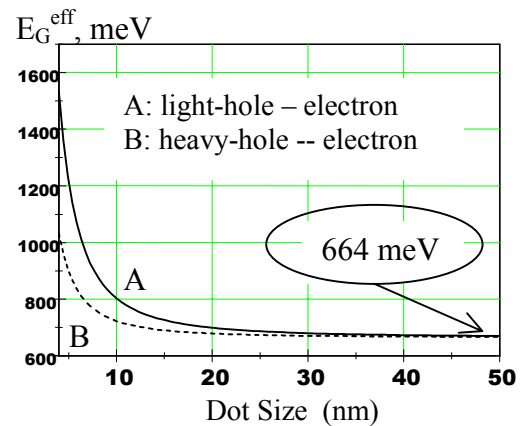


Figure 5. Calculated effective band-gap of the QD layers, e.g. the energy of the transition 1e-1h, as a function of the dot size. The controlled dot size variation allows one to cover the entire PV-important light frequency range.

3. ACHIEVING THE HIGH PV-CELL EFFICIENCY

The ultimate goal of the PV cell design is to maximize the efficiency $\eta = P_m/P_I$ (where P_m is the maximum power and P_I is the power of the incident light) of the cell and the solar power module. The standard equation for the PV cell efficiency can be written as

$$\eta = \frac{\left[\int_0^{\lambda_g} P(\lambda) d\lambda \right]}{\left[\int_0^{\infty} P(\lambda) d\lambda \right]} \frac{\left[\frac{E_G}{o} \int_0^{\lambda_g} N(\lambda) d\lambda \right]}{\left[\int_0^{\infty} P(\lambda) d\lambda \right]} \left[\frac{A_f}{A_t} \right] [1 - R] \eta_d \eta_{coll} \left[\frac{qV_{oc}}{E_G} \right] FF. \quad (1)$$

Here the first set of brackets [...] represent the loss by the long wavelengths, e.g. photons with energies $P(\lambda)$ less than the effective band-gap; the second [...] is the loss by the excess energy of the photons that dissipates as heat. The third [...] is the loss by the metal coverage and the fourth is the loss by the reflection. R is the reflection coefficient, η_d is the loss by the incomplete absorption, η_{coll} is the loss due to the recombination, which is related to the collection efficiency. The last two terms are the voltage factor and the fill-factor FF . It is clear that some of these factors, particularly those related to the absorption, recombination and reflection, can be directly enhanced by quantum confinement in the QDS i-layer. The tuning of the effective band-gap (transition energy between the first confined hole level $1h$ and the first electron level $1e$) via the dot size can be done in a very wide range (see Figure 5). The controlled QD size variation allows one to cover the PV-relevant light frequency range and tune to the optimum band gap for a given set of parameters. As described by [20] the alloy composition variation (for example in $\text{Si}_x\text{Ge}_{1-x}$ system) provides additional degree of E_G control.

It has been shown theoretically [8] that formation of mini-bands in QDS would have tremendous effect on the charge carrier transport in such structures with consequences for the electronic, photovoltaic and thermoelectric applications. Indeed the mini-band transport regime is characterized by much greater mobility than the electron hopping or single dot tunneling regimes. Optimization of the mini-bands, i.e. increasing the mini-band width along certain directions, achieving desired carrier effective mass, etc., may lead to further increase of the PV efficiency. The enhancement of the PV efficiency up to ~70% has been predicted while considering different energy conversion mechanisms [4, 31, 12], [17, 33]. It was pointed out that the mini-band formation may help in two ways: achieving the sub-gap absorption [4] and improving the carrier transport, correspondingly increasing the collection efficiency. The PV modeling software has to be able to capture both mechanisms essential for the PV cell efficiency enhancement. The comprehensive NanoTCAD-based device simulator, which we develop, uses 3D theoretical models for QDS described in [26, 27]. The model developed in Balandin group has been used for simulation of the carrier transport in Si QDS PV structures by the leading photovoltaic researchers, e.g. Green group in Australia [13].

3.1. Conditions for Mini-Band Formation in QDS

There have been a number of proposals of the solar cell applications of QDs [6, 7, 38]. The exact mechanism of the PV efficiency enhancement varies in different proposals. The assessment of the photovoltaic efficiency requires understanding of the absorption and carrier transport in these nanostructured materials. Physical properties of individual semiconductor QDs have been extensively studied both theoretically and experimentally [51]. The effects of the size, shape, strain fields, Coulomb interaction and dielectric screening on electronic states and optical response of individual quantum dots are addressed in literature in sufficient detail [9, 10, 30]. In a simplified picture, transport properties of arrays of weakly coupled quantum dots can be described in terms of hopping conduction, while optical response is defined by the energy spectrum of individual dots and inhomogeneous broadening due to the size distribution. For PV cell applications a more interesting case is strongly coupled QDs with small inter-dot distance QDS. Regimentation, i.e., ordering of QDs in one or more directions, makes the structure even better. Based on our analysis, the best PV cell operation can be achieved when the strong inter-dot coupling with substantial wave function overlap among the dots leads to the formation of two-dimensional (2D) or three-dimensional (3D) extended mini-bands instead of localized electronic states. Such energy spectrum modification is expected to take place provided that (i) the periodicity of QDs in the array is very high; (ii) the QD size is rather homogeneous; (iii) the inter-dot distance is small; and (iv) the dots are crystalline and with relatively low surface defect concentration. One should note here that the term “quantum dot superlattice” (unlike the term “quantum well superlattice”) does not imply perfect periodicity of quantum dots. Conventionally it only implies periodicity in layers of quantum dots but does not make an assumption about the in-plane

quantum dot distribution. Thus, in the discussion below we will use the term “regimented” QDS when we want to emphasize the periodicity of the dot distribution within each layer [Lazarenkova and Balandin, 2002].

Literature analysis shows that regimented or partially regimented 2D and 3D QDS have been fabricated by a variety of techniques [5, 30, 36, 43]. Electrochemically self-assembled 2D arrays of quantum dots in alumina templates are characterized by high degree of periodicity but by little wave function overlap [7]. Multiple arrays of Ge dots on Si grown by molecular beam epitaxy (MBE), on the other hand, are good candidates for mini-band formations although the dots in these structures are only partially regimented [30, 36]. A successful synthesis of 3D regimented QDs has also been reported [41, 42]. Regimentation, i.e. spatial site correlation in such structures, along all three directions brings an analogy with bulk crystals. In these artificial crystals the role of atoms is played by the quantum dots. Our preliminary study and data reported in literature indicate that the mini-band formation can be achieved in QD arrays, which are far from being absolutely perfect in terms of the surface quality and size dispersion. For example, Artemyev et al. [2, 3] demonstrated experimentally an evolution of the electron states from the individual to mini-band states in a dense QD ensemble that consisted of small CdSe dots with the average radius of $R \sim 1.6 \text{ nm} - 1.8 \text{ nm}$. Song et al. [40] investigated in-plane photocurrent in self-assembled InGaAs/GaAs QD arrays. They have reported that samples with inhomogeneous QD sizes show hopping conduction indicating the localization of carriers in individual dots, while the ordered and size-homogeneous QD arrays exhibit negative differential conductance that has been attributed to the carrier energy mini-band formation [27].

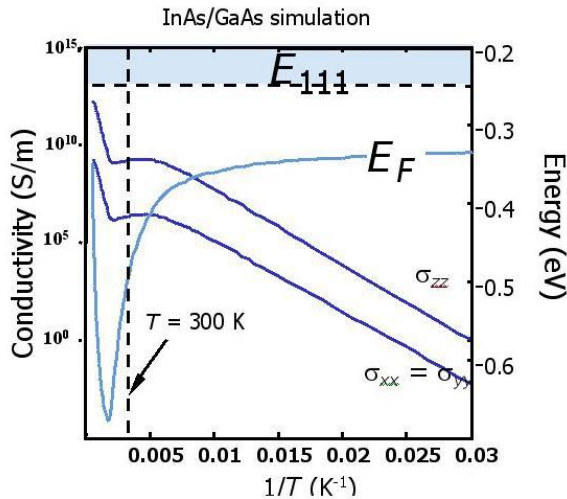


Figure 6. Simulated electrical conductivity (left axis) in InAs/GaAs QDS as a function of the inverse temperature. The right axis allows one to track the energy change: E_{111} denotes the edge of the lowest mini-band for the electrons in the conduction band while E_F indicates the position of the Fermi level. The calculations based on the model developed by Lazarenkova and Balandin [26] are in good agreement with experimental data reported BY Yakimov et al in [49,50].

In Figure 6 we present the results of the calculations of the electrical conductivity in InAs/GaAs QDS suitable for PV cell applications performed using the model developed in [26]. The calculations have been carried out under the assumption of the mini-band formation. The carrier mini-bands have been determined from the solution of the Schrödinger equation [27]. The results are presented as a function of the inverse temperature in order to facilitate the comparison with the measurements. The results of the simulation are in good agreement with available experimental data [9, 10, 49, 50].

3.2. Experimental Investigation of Carrier Transport in QDS

Figure 7 shows an SEM image of the GeSi/Si QDS, which was characterized at UCR in order to establish the nature of the carrier transport in such structures: band conduction type vs. hopping type. The obtained experimental data indicates that the Hall mobility is on the order of $150 \text{ cm}^2/\text{Vs} - 300 \text{ cm}^2/\text{Vs}$ at room temperature. The mobility values increase with decreasing temperature. The relatively high values of the mobility and its temperature dependence allowed us to conclude that the carrier transport is of the band conduction type (with mobility following the $\mu \sim T^{-3/2}$ law) rather than the electron (hole) hopping type with the electrical conductivity following the $G \sim G_0 \exp\{- (T_0/T)^x \}$ law (see Figure 8). It

is still an open question if this is a true mini-band transport or above-the-barrier transport due to the thermally excited carriers or the carrier band transport through the wetting and barrier layers [10].

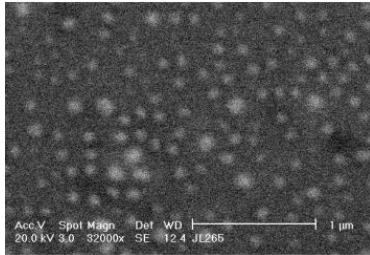


Figure 7 : SEM micrograph of the prototype GeSi/Si QDS. Experimental mobility data measured for this QDS was used for the theoretical model and simulation tool validation.

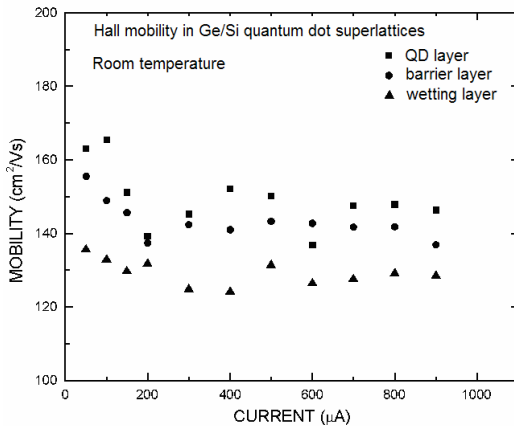


Figure 8: Experimental data on the room temperature Hall mobility measurements in GeSi/Si QDS conducted at UCR. The results are shown for the three different locations of the delta-doping: inside the quantum dot layer (marked with rectangulars); inside the barrier layer (marked with circles) and inside the wetting layer (marked with triangulars). Hall mobility is on the order of 150 cm²/Vs. The mobility values increase with decreasing temperature (1600 to 3000 cm²/Vs at 77K).

4. RADIATION HARDNESS OF QUANTUM DOT STRUCTURES

The results of our preliminary research and analysis of the available data on the radiation hardness of solar cells indicate that the radiation tolerance of the QD-based solar cells can be up to two orders of magnitude higher than that of the conventional solar cells. Although the exact mechanism of the radiation hardness improvement in nanostructured materials is not known yet, there have been a number of reports on the optoelectronic devices with QDs in the active area, which demonstrated the increased radiation tolerance [16, 19, 22, 29, 34, 35]. Klimeck [24] suggested that QDs offer an attractive radiation hard solid state technology for the sensor applications important for future space missions. In [39] the influence of the 2 MeV electron irradiation on the photoluminescence from InAs/GaAs QD and quantum well (QW) structures has been compared. A superior radiation hardness of the QDs has been established and attributed to the different influence of the defects created inside the QWs and QDs and in the adjacent GaAs barrier within the tunneling distance.

Some of the fundamental properties of QDs suggest that optoelectronic devices incorporating QDs could tolerate greater radiation damage than other heterostructures [29]. One of them is based on a simple geometrical argument: the total volume percentage of the active QD region is very small. Specifically, in the self-assembled InGaAs/GaAs QDs the surface coverage range from 5% to 25% depending on the growth conditions [28]. Therefore, the chance of finding the radiation-induced defects in the active region is reduced. In addition, the exciton localization in QDs due to 3D confinement (InGaAs dots have an average 5 nm height and 25 nm diameter) reduces the probability of the carrier non-radiative recombination at the radiation induced defect centers. In [29], the authors compared the optical emission from InGaAs QW and QD structures after the controlled irradiation with 1 MeV protons. The experiment has shown the improved radiation hardness of QDs. These results [29] have been interpreted in such a way that QD structures are

inherently more radiation tolerant due to the effects of 3D quantum confinement. An increase in the radiation hardness of as much as two orders of magnitude has been observed by comparisons with QWs of the same composition and placed at the same depth in the structure.

The radiation effects in polymer photodetectors (PPD) using InP QDs, and the role of nanostructures and QDs in PPD and solar cells have been studied by Taylor *et al.* [44, 45]. Pre- and post- irradiation responses of electrostatically self-assembled (ESA) grown polymer detectors using InP QDs have been examined for photovoltage degradation and aging. The data indicates an excellent potential for developing polymer based photonic devices with increased radiation resistance suitable for transition to photonic space applications, compared to devices without QDs, studied in [46, 47].

5. NanoTCAD - INTEGRATED SOFTWARE TOOLS FOR QDS-BASED PV APPLICATIONS

The PV-related models discussed above are being integrated within the advanced software tool NanoTCAD, which is a 3D device simulator developed and commercialized by CFD Research Corporation [14]. This integration provides a user-friendly interface and a large database of the semiconductor material properties available in NanoTCAD. It also makes possible a complete PV-cell simulation including both quantum and classical models for the appropriate PV-cell elements, both DC and transient regimes, etc. The models are currently being extended to incorporate simulation of the electron-phonon transport in QDS made of semiconductors with both cubic and hexagonal crystal lattice, e.g., InAs/GaAs, Ge/Si, CdSe, ZnO. The NanoTCAD with PV feature will be used to accurately simulate electron (hole) and exciton states, phonon dispersion and absorption coefficients in superlattices with the arbitrary dot shape as well as in other nanostructured materials. The material properties database is being extended to include new ones, which are important for the space solar cells. To account for the effects of extreme environments (temperature effects and space radiation) on the QDS-solar cell, the coupled solution for all physical phenomena (quantum carrier transport, phonon transport, drift diffusion model and thermal model) is implemented within NanoTCAD. This new modeling and simulation tools will help to better understand and predict behavior of nanostructured solar cells, nano-devices and novel materials in space environment, and reduce the amount of testing cost and time.

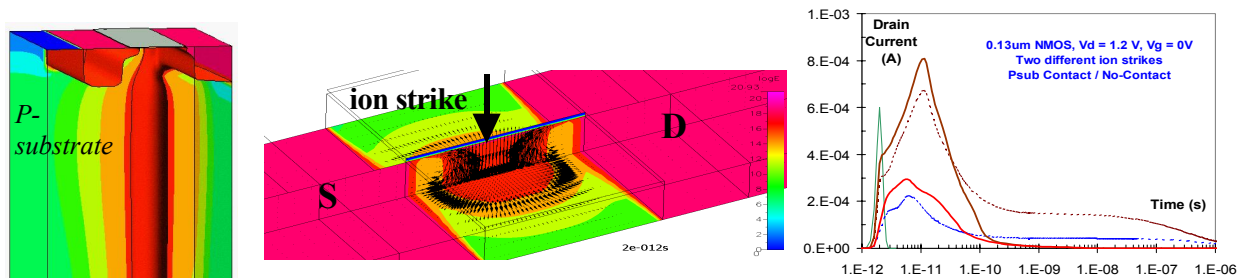


Figure 9. Sample results of CFDRC 3D simulations of space radiation effects (in this case: an ion strike, called single event) in nano-scale semiconductor devices: a 3D ion-track model (left), current flow vectors and electron density (color map) at $t = 2$ ps after ion strike (middle), and computed currents of the off-transistor for two different ion strikes (right).

An example of our 3D simulation of the space radiation effect on semiconductor device is shown in Figure 9. The software allows to capture features of a single ion strike and predict the device performance depending on the total radiation dose and the dose-rate. CFDRC has developed an adaptive dynamic 3D mesh generation capability to allow complex, multi-branched track data generated by Vanderbilt University's Geant4-based Monte-Carlo Radiation Energy Deposition (MRED) [25, 52] simulations to be incorporated into NanoTCAD [15, 48] for performance of transient device response simulations (see Figure 10).

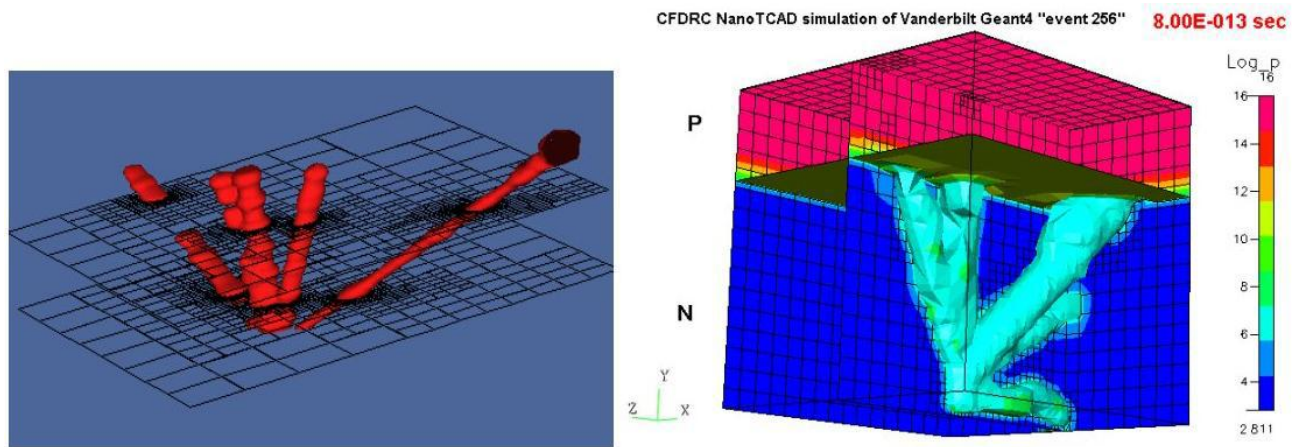


Figure 10. Adaptive 3D mesh refinement in the vicinity of the radiation event tracks is shown in the different plane cross-sections; (b) Radiation event in p-n diode ($4 \times 4 \times 4 \mu m^3$). Snapshots of 3D distribution of the local hole density $\log(p)$, for $t = 0.8 ps$. The isosurface shows the level of $p = 10^6 / cm^3$.

The NanoTCAD simulator demonstrates an efficient use of computer memory and CPU time for large 3D problems. As an example, NanoTCAD simulator can solve a transient 3D multi-branched ion strike problem with 100,000 nodes mesh (300,000 unknowns) on a laptop with 512 MB memory. The memory size and CPU time depend almost linearly on the number of mesh nodes. Figure 11 shows a typical dependence of total memory and CPU time for NanoTCAD simulations of 3D devices using unstructured meshes. CFDRC NanoTCAD can solve a problem with 3D unstructured mesh for up to 500,000 nodes within 2GB memory.

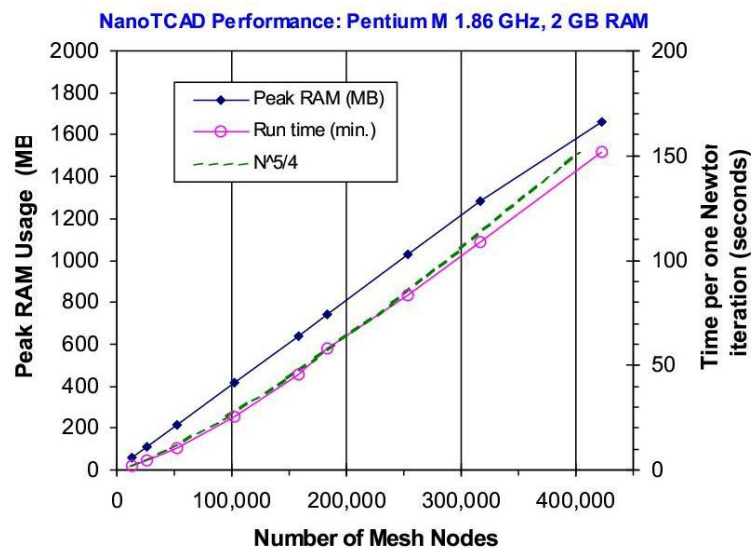


Figure 11. Total NanoTCAD simulator performance for modeling 3D devices: memory, solid curve with diamonds (in MB), and CPU time, solid curve with circles (in seconds, per Newton iteration) versus number of mesh nodes. One can see that the dependence is almost linear for both memory and CPU time, and close to theoretical estimate for the CPU time (dashed green curve).

6. CONCLUSIONS

We have outlined issues and problems encountered in the development of the quantum-dot based solar cells and comprehensive software tools for simulation and optimization of the nanostructure-based photovoltaic materials. Some experimental results used for the model validation have been reviewed. The novel modeling and simulation tools for the quantum-dot-based nanostructures will help to better understand and predict the behavior of the nano-devices and novel materials in space environment. We specifically discuss how the new models for the charge carrier transport in the quantum dot superlattices are integrated into the advanced photonic-electronic device simulator NanoTCAD.

Acknowledgement

The work has been supported, in part, by the NASA project NNC06CA83C. The authors thank Sheila Bailey, David Wilt and Seth Hubbard for illuminating discussions on photovoltaic cells. The authors are indebted to Edward W. Taylor for an opportunity to present an invited talk at the SPIE's International Symposium on Optics & Photonics, 13-17 August 2006, San Diego, CA.

REFERENCES

1. H. Amekura, N. Kishimoto, and K. Kono, "Radiation-induced Two-step Degradation of Si Photoconductors and Space Solar Cells", *IEEE Trans. on Nuclear Science* 45 (3), 1508 (1998).
2. M.V. Artemyev, A.I. Bibik, L.I. Gurinovich, S.V. Gaponenko, and U. Woggon, "Evolution from individual to collective electron states in a dense quantum dot ensemble", *Phys. Rev. B* 60, 1504 (1999).
3. M.V. Artemyev, U. Woggon, H. Jaschinski, L.I. Gurinovich, and S.V. Gaponenko, "Spectroscopic Study of Electronic States in an Ensemble of Close-Packed CdSe Nanocrystals", *J. Phys. Chem. B* 104, 11617 (2000).
4. S.G. Bailey, S. L. Castro, R. P. Raffaele, S. Fahey, T. Gennett, and P. Tin, "Nanostructured Materials for Solar Cells," 3rd World Conference on Photovoltaic Energy Conversion, May 11-18, 2003, Osaka, Japan
5. A.A. Balandin, S. Bandyopadhyay, P.G. Snyder, S. Stefanovich, G. Banerjee, and A.E. Miller, *Phys. Low-Dim. Structur.*, 11/12, 155 (1997).
6. A.A. Balandin, "Quantum dot-based solar cells," invited talk at the UCLA Nanotechnology Workshop, Las Vegas, July 2000.
7. AA. Balandin, K.L. Wang, N. Kouklin and S. Bandyopadhyay, "Raman spectroscopy of electrochemically self-assembled CdS quantum dots," *Applied Physics Letters*, 76, 137 (2000).
8. A.A. Balandin and O.L. Lazarenkova, "Mechanism for thermoelectric figure-of-merit enhancement in regimented quantum dot superlattices," *Applied Physics Letters*, 82, 415 (2003).
9. Y. Bao, A.A. alandin, Liu J.L., *et al.*, "Experimental investigation of Hall mobility in Ge/Si quantum dot superlattices," *Appl. Phys. Lett.* 84, 3355 (2004).
10. Y. Bao, W. L. Liu, M. Shamsa, K. Alim, A. A. Balandin, and J. L. Liub, "Electrical and Thermal Conductivity of Ge/Si Quantum Dot Superlattices", *Journal of Electrochemical Society*, 152 (6) G432-G435 (2005).
11. J.P. Benner and Kazmerski L., "Photovoltaics gaining greater visibility," *IEEE Spectrum*, p. 34 (Sep.1999).
12. A.S. Brown, M.A. Green and R.P. Corkish, "Limiting efficiency for a multi-band solar cell containing three and four bands", *Physica E* 14, 121 (2002).
13. J. Chu-Wei and Martin A. Green, (2006), "Silicon quantum dot superlattices: Modeling of energy bands, densities of states, and mobilities for silicon tandem solar cell applications, *J. Appl Phys.* 99, 114902 (2006).
14. CFDRRC (2006) NanoTCAD web site: http://www.cfdrcc.com/bizareas/microelec/micro_nano/

15. A. I. Fedoseyev, M. Turowski, and M. S. Wartak, "Kinetic and Quantum Models in Simulation of Modern Nanoscale Devices", chapter In: *Handbook of Semiconductor Nanostructures and Devices*. Edited by A.A. Balandin and Kang L. Wang, American Scientific Publishers, Los Angeles (2006).
16. A. Fijany, Klimeck G., Leon R., Qiu Y., Toomarian N., "Quantum Dots Based Rad-Hard Computing and Sensors", *Forum On Innovative Approaches To Outer Planetary Exploration 2001–2020*, Feb. 21–22, 2001 Lunar and Planetary Institute, Houston, Texas.
17. M.A. Green, "*Silicon Solar Cells: Advanced Principles and Practice*", Bridge Printery, Sydney, 1995;
18. M.A. Green, "Photovoltaic Applications of Nanostructures", in *Handbook of Semiconductor Nanostructures and Nanodevices* (ASP, Los Angeles, 2006) edited by A.A. Balandin and K.L. Wang.
19. F. Guffarth, R. Heitz, M. Geller, C. Kapteyn, H. Born, R. Sellin, A. Hoffmann, and D. Bimberg, "Radiation hardness of InGaAs/GaAs quantum dots", *Appl. Phys. Lett.* 82, 1941 (2003).
20. S. Guha, J. Yang, "Science and technology of amorphous silicon alloy photovoltaics", *IEEE Tr. ED*, vol. 46(10), 2080-2085; A Shah, *et al.*, *Material Science Engineer.*, B69-70, 219 (2000); R.S. Mane *et al.*, *Material Chemistry Phys.* 60, 196 (1999).
21. S. Hazra, S. Ray, "Nanocrystalline silicon as intrinsic layer in thin film solar cells", *Solid State Communicat.*, 109(2), 125-128 (1999).
22. M.B. Huang, J Zhu, S Oktyabrsky, "Enhanced radiation hardness of photoluminescence from InAs quantum dots embedded in an AlAs/GaAs superlattice structure", *Nuclear Instrum. Meth. in Phys. Research B* 211, 505 (2003)
23. R. R. King, C. M. Fetzer, P. C. Colter, K. M. Edmondson, J. H. Ermer, H. L. Cotal, H. Yoon, A. P. Stavrides, G. Kinsey, D. D. Krut, N. H. Karam, "High-Efficiency Space and Terrestrial Multijunction Solar Cells Through Bandgap Control in Cell Structures", *29th IEEE PVSC*, May 20-24, 2002, New Orleans, Louisiana.
24. G. Klimeck, "NASA Relevance for Nanoelectronic Modeling", available online: http://dynamo.ecn.purdue.edu/~gekco/nemo3D/NASA_relevance_3D.html
25. A. S. Kobayashi (2004), A. L. Sternberg, Lloyd W. Massengill, R. D. Schrimpf, Fellow, and Robert A. Weller, Spatial and Temporal Characteristics of Energy Deposition by Protons and Alpha Particles in Silicon, *IEEE Trans. Nucl. Sci.*, 51, 3312, Dec. 2004
26. O. Lazarenkova and A. Balandin, "Mini-band formation in quantum dot superlattices," *J. Appl. Phys.*, 89, 5509 (2001).
27. O. Lazarenkova and A. Balandin, (2002) "Electron and phonon energy spectra in a three-dimensional regimented quantum dot superlattice", *Phys. Rev. B* 66, 245319 (2002)
28. R. Leon, D. R. M. Williams, J. Krueger, E. R. Weber and M. R. Melloch, "Diffusivity transients and radiative recombination in intermixed In_{0.5}Ga_{0.5}As/GaAs quantum structures", *Phys. Rev. B* 56, R4336.
29. R. Leon, G.M. Swift *et al.*, "Changes in luminescence emission induced by proton irradiation: InGaAs/GaAs quantum wells and quantum dots", *Appl. Phys. Lett.* 76 (15), 2075 (2000).
30. J.L. Liu, W.G. Wu, A. Balandin, and K.L. Wang, *Appl. Phys. Lett.* 75, 1745 (1999); J.L. Liu, W.G. Wu, A. Balandin, G.L. Jin, and K.L. Wang, *Appl. Phys. Lett.* 74, 185 (1999).
31. A. Luque and Marti A., "Increasing the Efficiency of Ideal Solar Cells by Photon Induced Transitions at Intermediate Levels", *Phys. Rev. Lett.* 78 (26), 1997, 5014 (1997).
32. S. R. Messenger, G. P. Summers, E. A. Burke, R. J. Walters, and M. A. Xapsos, "Modeling solar cell degradation in space: A comparison of the NRL displacement damage dose and the JPL equivalent fluence approaches," *Progress in Photovoltaics: Res. Applicat.* 9, 103 (2001).
33. A. Nozik, "Quantum dot solar cells", *Phys. E: Low-dimensional Systems and Nanostructures* 14(1-2), 115 (2002).
34. P.G. Piva, *et al.*, "Enhanced Degradation Resistance of Quantum Dot Lasers to Radiation Damage", *Appl. Phys. Lett.* 77, 624 (2000).

35. C. Ribbat, R. Sellin, M. Grundmann, D. Bimberg, N.A. Sobolev, and M.C. Carmo, "Enhanced radiation hardness of quantum dot lasers to high energy proton irradiation", *El. Lett.* 37,174 (2001).
36. P.C. Sharma, K.W. Alt, D.Y. Yeh, D. Wang, K.L. Wang, *J. Electron. Materials* 28, 432 (1999).
37. P.R. Sharps, C.H. Thang, P.A. Martin, and H. Hou, "Proton and Electron Radiation Analysis of GaInP₂/ GaAs Solar Cells", *Progress in Photovoltaics: Research and Applications. Special Issue: Advances in Space Photovoltaics* 10(6) , 383 (2001/02).
38. S. Sinharoy, King, C.W. Bailey, S.G. Raffaele, R.P. "InAs Quantum Dot development for enhanced InGaAs space solar cells," *Proc. Photovoltaic Specialists Conference, IEEE*, 3-7 Jan 2005, 94.
39. N.A. Sobolev, A. Cavaco, M.C. Carmo, M. Grundmann, F. Heinrichsdorff, D. Bimberg, "Enhanced radiation hardness of InAs/GaAs quantum dot structures", *Phys. Stat. Sol.B* 224, 93 (2001).
40. H.Z. Song , K. Akahane, S. Lan, H.Z. Xu, Y. Okada, and M. Kawabe, "In-plane photocurrent of self-assembled In(x)Ga(1-x)As/GaAs(311)B quantum dot arrays", *Phys. Rev. B* 64, 085303 (2001).
41. G. Springholz , V. Holy, M. Pinczolits, and G. Bauer, "Self-Organized Growth of Three- Dimensional Quantum-Dot Crystals with fcc-Like Stacking and a Tunable Lattice Constant", *Science* 282, 734 (1998).
42. G. Springholz, M. Pinczolits, P. Mayer, V. Holy, G. Bauer, H.H. Kang, and L. Salamanca-Riba, "Tuning of Vertical and Lateral Correlations in Self-Organized PbSe/Pb1-xEuxTe Quantum Dot Superlattices", *Phys. Rev. Lett.*, 84, 4669 (2000)
43. T. Takagahara," Effects of dielectric confinement and electron-hole exchange interaction on excitonic states in semiconductor quantum dots", *Phys. Rev. B* 47, 4569 (1993).
44. E. W. Taylor, J.Nichter, F.Nash et al, "Radiation resistant polymer-based photonics for space applications", *Proc. SPIE*, 5554, 15 (2004).
45. E. W. Taylor, "The role of nanostructures and quantum dots in detectors and solar cells for radiation hardened space applications", *SPIE*, 6308, August 2006.
46. E. W. Taylor, D. Le, M. F. Durstock et al, "Space Radiation Induced Effects in Polymer Photo-Detectors", *Proc. SPIE*, 4823, July 2002.
47. E. W. Taylor, "Interaction and responses of linear and nonlinear optic polymer based photonic materials and devices with ionizing radiation", *Proc. SPIE*, 5897, August 2005.
48. M. Turowski, A. Raman, and R. Schrimpf, "Non-Uniform Total-Dose-Induced Charge Distribution in Shallow-Trench Isolation Oxides", *IEEE Trans. on Nuclear Science* 51, 3166 (2004).
49. A.I. Yakimov, A. V. Dvurechenski, A. I. Nikiforov, and O. P. Pchelyakov, "Negative Interband Photoconductivity in Ge/Si Heterostructures with Quantum Dots of the Second Type", *J. Appl. Phys.* 89, 5676 (2001).
50. A.I. Yakimov, V. A. Markov, A. V. Dvurechenski, and O. P. Pchelyakov, " Longitudinal conductivity of Ge/Si heterostructures with quantum dots", *JETP Lett.* 63, 444 (1996).
51. K.L. Wang and Balandin A., *Quantum Dots: Physics and Applications*, in *Optics of Nanostructured Materials*, New York: Wiley & Sons, August 2000, 515 (2000).
52. R. A. Weller, A. L. Sternberg, L.W. Massengill, R. D. Schrimpf, and D. M. Fleetwood, "Evaluating average and atypical response in radiation effects simulations", *IEEE Trans. Nucl. Sci.* 50, 2265 (2003).